

Photocatalytic water splitting using hygroscopic MgO modified TiO₂/WO₃ dual-layer photocatalysts

Chao-Wei Huang^{*,†}, Chi-Hung Liao^{**,***}, and Jeffrey Chi-Sheng Wu^{**,†}

^{*}Department of Chemical and Materials Engineering, National Kaohsiung University of Science and Technology, Kaohsiung 80778, Taiwan

^{**}Department of Chemical Engineering, National Taiwan University, Taipei 10617, Taiwan

^{***}Institute of Nuclear Energy Research, Atomic Energy Council, Lungtan 32546, Taiwan

(Received 14 March 2020 • Revised 11 May 2020 • Accepted 4 June 2020)

Abstract—MgO modified TiO₂/WO₃ dual-layer photocatalysts (DLP) was synthesized by radio-frequency magnetron sputtering (RFMS). The influences of MgO on the properties and the performance of the prepared DLP were investigated. MgO modified TiO₂ thin films were characterized by instrumental analysis such as XRD, AFM, SEM-EDS, and UV-visible absorption spectrometry. Their photoactivity was assessed by conducting photovoltammetry followed by splitting water in a twin-cell reactor, where hydrogen gas and oxygen gas were produced separately. The yield of H₂ and O₂ in the twin-cell reactor corresponded to the photovoltammetry results, indicating that MgO can significantly improve the photoactivity of DLP. The improvement is attributed primarily to the hygroscopic *Nature* of MgO, which can increase the amount of H₂O molecules on the surface of TiO₂ for carrying out the photoreaction. In addition, the incorporated MgO layer can also act as an insulator to suppress the electron leakage that occurred at the TiO₂-water interface.

Keywords: Photocatalyst, Water Splitting, Solar Hydrogen, Rf Magnetron Sputtering, MgO

INTRODUCTION

Due to the issues of global warming and energy shortage, scientists worldwide are searching to find alternative energies to replace fossil fuel [1]. For an ideal fuel, hydrogen is regarded as an excellent candidate since it has high energy density, no environmentally harmful issues, and is plentiful on earth. However, most of the commercial hydrogen that we use today is still derived from fossil fuels via steam reforming [2]. An example is the conversion of methane (CH₄) to hydrogen gas (H₂) by Ni-loaded alumina catalyst at high temperature. Such a process has high energy consumption and the release of carbon dioxide (CO₂). Therefore, water splitting via photocatalysis, which can convert light energy, particularly sunlight, into chemical energy such as H₂ in the presence of photocatalysts, provides a potential strategy for clean and inexpensive production of H₂ [3,4]. The produced H₂ can be used by a fuel cell or hydrogen engine and converted back to water, making its life cycle clean and sustainable.

The mechanism of photocatalytic water splitting basically involves three basic steps: (1) the generation of electron-hole pairs at the photocatalyst upon absorbing light with energy greater than its bandgap, (2) the oxidation of water by photo-generated holes to produce O₂ and protons (H⁺), and (3) the reduction of protons by photo-generated electrons to form H₂. Over the past few years, TiO₂ (titanium dioxide) has been the most extensive photocatalyst to conduct photocatalytic water splitting due to its stability, economics,

and environmentally friendly properties [5]. However, reactions involving TiO₂ may encounter problems such as the recombination of photo-generated electrons and holes and the backward reaction of H₂ and O₂ to form water. In addition, pristine TiO₂ cannot absorb visible light since its bandgap is around 3.20 eV, which corresponds only to the UV region of the solar spectrum. To improve the performance of photocatalytic water splitting, enormous research in visible light-absorbing photocatalysts [6-9] as well as efficient photoreactor systems [10,11] is developed sustainably. Previously, we reported a novel dual-layer photocatalysts (DLP) to conduct water splitting in a twin-cell (H-type) reactor under visible-light irradiation [12,13]. The photocatalyst was comprised of a Ti foil sandwiched by a dual-layer visible light-absorbing photocatalyst (made up of a visible light-absorbing TiO₂ and a visible light absorbing WO₃) and a Pt cathode. The purpose of adopting a dual-layer structure is to improve the light absorption efficiency of the photocatalyst since TiO₂ and WO₃ thin films will absorb different parts of the visible-light spectrum. Such configuration also benefits the charge separation of the photocatalyst since the conduction band of WO₃ is lower than that of TiO₂, while the valence band of TiO₂ is higher than that of WO₃. Thus, WO₃ serves as an electron pool, while TiO₂ is regarded as a hole pool. A twin-cell reactor consisted of two compartments (half reactors), which were separated by a Nafion membrane and the photocatalyst to allow only the transport of protons across the two compartments [14]. Therefore, when the photocatalyst anode was irradiated by visible light, water oxidation occurred at the anode to give O₂ and protons, while the reduction of protons occurred at the cathode to give H₂, resulting in separate evolution of H₂ and O₂. The simultaneous separation of evolved H₂ and O₂ during photoreaction has the merits of eliminating back-

[†]To whom correspondence should be addressed.

E-mail: cswu@ntu.edu.tw, huangcw@nkust.edu.tw

Copyright by The Korean Institute of Chemical Engineers.

ward reaction of H₂ and O₂ to form water, preventing the possible explosion of the H₂-O₂ gas mixture, and reducing the cost for the additional separation process.

The coating of electrically isolate thin-films, for example, magnesium oxide (MgO) and silicon dioxide (SiO₂) on nanocrystalline TiO₂ particles, will improve TiO₂'s photocatalytic performance [15]. Tada et al. reported that the MgO coating on TiO₂ causes an increase of TiO₂'s photocatalytic activity by three times to decompose cationic surfactants [16]. Likewise, Anderson and Bard demonstrated the coating of an electrically isolating SiO₂ layer on TiO₂ would improve its photocatalytic performance in the degradation of RG-6 dye by comparing the bare TiO₂ [17]. The enhanced photocatalytic activity of the photocatalysts was attributed to the improved adsorption because of the oxide-layer coating. Furthermore, Jung et al. reported the preparation of TiO₂-MgO core-shell-structured nanoparticles for the photodegradation of organic contaminants [18]. Comparing the bare TiO₂, it was found that the ultrathin film of MgO with high porosity on TiO₂ has numerous OH groups and H₂O molecules, leading to an improvement of its photocatalytic activity. To investigate the role of metal oxide layer, Bae et al. prepared a MgO layer on TiO₂/ITO electrode to conduct photoelectrochemical water splitting [19]. They found that the MgO layer would block the transfer of charge carriers between TiO₂ and electrolyte. It exhibited both a positive effect of preventing the back electron transfer as well as the negative effect of preventing the hole escape. Due to the competition of dual effects, the thickness of MgO layer should be optimized. However, applying a bias voltage on the design photoelectrode would favor the negative effect, leading to poorer performance. Therefore, a better strategy to utilize the positive effect of MgO layer is to conduct water splitting via photocatalysts, instead of applying an external bias voltage in the photoelectrochemical cell.

We investigated the effects of MgO on the performance of dual-layer photocatalysts. Various MgO modified TiO₂ thin films were first fabricated by radio-frequency magnetron sputtering (RFMS). Then, the prepared thin films were characterized by AFM, SEM-EDS, XRD, and UV-visible spectrometry to analyze their morphology, elemental characterization, crystallinity, and optical absorption. The photocatalytic activity of these prepared thin films under UV light irradiation was examined by photovoltammetry. The mechanism of the enhancement on the photocatalytic activity of MgO modified photocatalysts was also proposed. Consequently, MgO modified DLP was employed to split water via photocatalytic reaction under visible light irradiation in a dual-cell reactor, where hydrogen and oxygen were produced separately [20].

EXPERIMENTAL

1. Synthesis of TiO₂, WO₃ and MgO Thin Films by Sputtering

All thin films of the samples were fabricated by RFMS. Before sputtering, ITO (indium tin oxide, Merck, 20-30 Ω/cm²) glass employed as substrate was under ultrasonic cleaning by DI-water, acetone, methanol, and isopropanol, followed by drying at 110 °C for one hour. Then, the ITO was placed in a vacuum chamber for sputtering. The distance of ITO and target was 60 mm, and the target plates included TiO₂, WO₃, and MgO (grade 99.99%), pro-

vided by Solar Applied Materials Technology Corp. The Ti foil (99.7%, 0.127 mm thick), obtained from Uni-Onward Corp., was also adopted as the substrate for conducting a water-splitting reaction. To carry out the procedures of sputtering deposition, the based pressure of the vacuum chamber was controlled at 9×10⁻⁶ torr initially. After that, argon gas (grade 99.999%) was introduced at the flow rate of 40 sccm, and the working pressure was fixed at 16 mtorr. During sputtering, the power was set at 250, 200, and 75 W for depositing TiO₂, WO₃, and MgO thin film, respectively, which area was 1 cm×2 cm. To prepare TiO₂ and WO₃ thin films with visible-light absorbance (i.e., vis-TiO₂ and vis-WO₃), the sputtering temperature was increased to 773 K, while the deposition of MgO was performed at 623 K. The deposition rate for TiO₂, WO₃, and MgO was 80, 720, and 14 nm/hr, respectively, which was determined from the pre-constructed sputtering time vs. thickness calibration curve. To investigate the effect of MgO on DLP, varied amount of MgO (2, 10, 30, 80 nm) was deposited on the prepared TiO₂ thin films (thickness of 1,120 nm). The MgO modified TiO₂ thin film with 0, 2, 10, 30, and 80 nm of MgO was named as bare_TiO₂, MgO(2)_TiO₂, MgO(10)_TiO₂, MgO(30)_TiO₂, and MgO(80)_TiO₂, respectively. Since the MgO deposited on TiO₂ was extremely thin, it was difficult to perform direct measurement using a conventional stylus profiler. Therefore, the thickness of MgO on TiO₂ was estimated from the deposition time based on the calibration curve constructed for MgO.

2. Characterization of the Prepared Thin Films

The thickness of thin films prepared in this study was measured by the XP-2 Stylus Profiler (Ambios Technology). The scan speed, scan length, and stylus force was 0.1 mm/s, 2-3 mm, and 5 mg, respectively. The X-ray diffraction (XRD) analysis of the thin films fabricated in this study was examined by D8-ADVANCE (Bruker). The scanning angle (2θ) was between 20-80°, using X-ray radiation of Cu Kα (1.5418 Å). The measurement was conducted under 'Detector Scan' mode, in which the X-ray source was kept still at an angle of 3°, while the detector moved at a rate of 1°/min. Since the thin films prepared in this study were transparent, they were all measured under the absorption (transmission) mode by the Evolution 600 UV-Vis absorption spectrometer (Thermo Scientific). The scanning range of wavelength was between 350-700 nm at a rate of 4 nm/s. Before measurement, thin-film was first deposited on ITO glass, and then it was measured together with the ITO glass. In order to eradicate the absorption interference of ITO glass, the baseline measurement was carried out by using bare ITO glass; therefore, absorption solely from the deposited thin film can be achieved. The surface morphology of the thin films prepared in this study was observed by using a field emission scanning electron microscope (FE-SEM, Hitachi-S4800) with an electron beam energy of 15 kV and the working distance of approximately 8 mm. Elemental characterizations of the photocatalytic thin films were analyzed by the EDS system that was incorporated with FE-SEM. NT-MDT NTEGRA Prima atomic force microscope (AFM) was adopted to analyze the surface roughness of the prepared thin films. Water contacting angle (WCA) was measured by using OSA60 (Ningbo NB Scientific Instruments).

3. Photocurrent Measurements

Photocurrent measurement is an important technique often

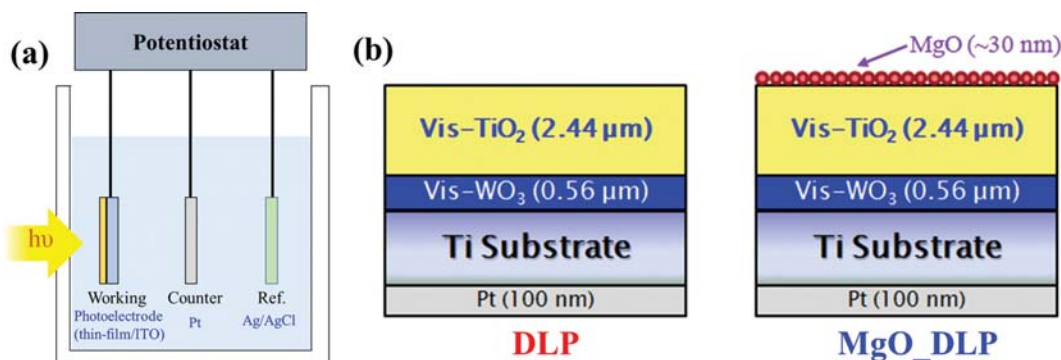


Fig. 1. (a) Photocurrent measurement setup, and (b) schematic diagram of DLP and MgO_DLP.

used to predict the performance (activity) of the photocatalyst before performing the actual photoreaction. The technique is based on the fact that no photoreaction will occur unless electron-hole pairs are generated upon light irradiation. If directed by a circuit, such photogenerated electron-hole pairs will create a current which can then be measured. In this study, the setup of photocurrent measurement was depicted, as shown in Fig. 1(a). Various thin-film coated ITO glasses served as the photoelectrodes. The working, counter, and reference electrodes were the prepared photoelectrode, Pt wire, and Ag/AgCl, respectively, which were immersed in KOH solution (1 M) as the electrolyte. For measuring the photocurrent produced under light irradiation, a potentiostat (AUTO-LAB PGSTAT302N) was used with the scanning voltages between -0.5 V~ 1.5 V. Since the TiO_2 photocatalyst prepared in this study was both UV and visible-light responsive, with UV absorption higher than visible light, UV light (100-W mercury lamp, HL400EH-5 SEN LIGHT Corp.) was employed to conduct the photocurrent measurements. The intensity of UV (365 nm) light, determined by measuring inside the container, was 3.2 mW/cm^2 .

4. Apparatus of Photocatalytic Water Splitting Reaction

For preparing the photocatalyst, dual-layer photocatalyst (DLP: vis- TiO_2 2,450 nm/vis- WO_3 550 nm) or MgO modified dual-layer photocatalyst (MgO_DLP: MgO 30 nm/vis- TiO_2 2,450 nm/vis- WO_3

550 nm) was first deposited on a Ti foil substrate. On the backside of Ti foil, Pt layer was also deposited by sputtering. Then, the structure of DLP or MgO_DLP/Ti/Pt (100 nm) was obtained, as shown in Fig. 1(b). Subsequently, the photocatalysts and a Nafion film (178 μm thick, Nafion-117 Aldrich) were sandwiched between two silicone rubber plates with two rectangular openings, respectively. The area dimension of each opening was $1\text{ cm} \times 2\text{ cm}$. This experimental module was clamped in a twin-cell reactor, filled with 0.05 M of NaOH solution and 0.025 M of H_2SO_4 solution for TiO_2 side and Pt side, respectively. The photocatalyst was irradiated by the simulated light of $100\text{ mW}/\text{cm}^2$, provided by a 300-W Xe lamp with AM 1.5G filter, as shown in Fig. 2. Then, TiO_2 side and Pt side can separately generate O_2 and H_2 , which were on-line collected and analyzed by a 1 mL sampling loop and a GC-TCD (China GC 2000) analyzer. Such a twin-cell reactor was also described in our previous study [21].

RESULTS AND DISCUSSION

Fig. 3 presents the SEM images of (a) bare- TiO_2 , (b) MgO(2)- TiO_2 , (c) MgO(10)- TiO_2 , (d) MgO(30)- TiO_2 , and (e) MgO(80)- TiO_2 under magnification of 50,000X. It appears that TiO_2 crystals exhibit less sharp edges as the thickness of MgO increases, particularly for MgO(30)- TiO_2 and MgO(80)- TiO_2 , suggesting the presence of MgO. Nevertheless, the MgO deposited cannot completely cover the TiO_2 surface. On the other hand, the MgO in MgO(2)- TiO_2 and MgO(10)- TiO_2 cannot be clearly observed. It is also interesting that the surface of TiO_2 crystals becomes brighter as the amount of MgO increases. This is believed to result from the increasing "charging effect" during SEM analysis, which was induced by the presence of the insulating material, MgO, on TiO_2 . In addition, the MgO-coated TiO_2 , as observed in the SEM image (Fig. 3(a)), shows a more pronounced surface texture on edge as compared to the pure TiO_2 (Fig. 3(d)). Therefore, it is reasonable to imply that the textures due to the MgO deposition may increase the roughness and the contacting surface area TiO_2 , leading to an enhancement of photocatalytic performance. As shown in Table 1, the results of EDS analysis exhibited the chemical composition of the fabricated MgO modified TiO_2 thin films. It is noted that the signal of Mg and O increases as the thickness of MgO increases, indicating the presence of MgO in MgO modified TiO_2 . On the other hand, the

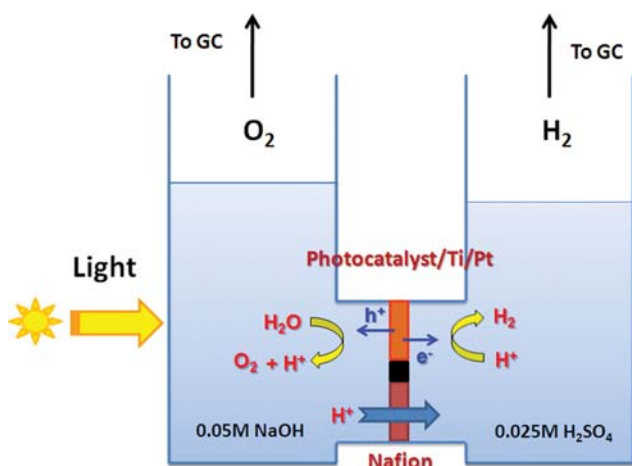


Fig. 2. H-type reactor for water splitting reaction.

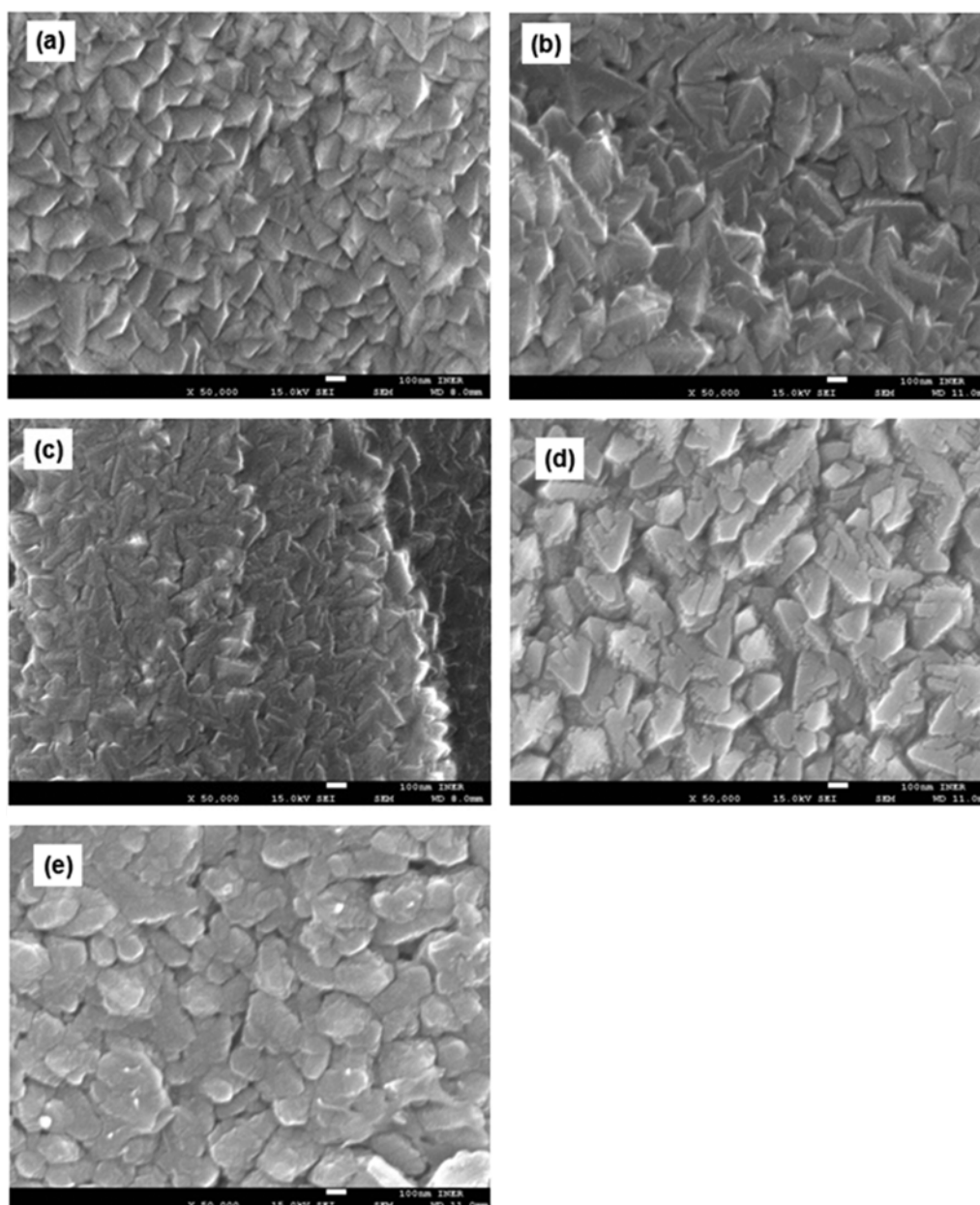


Fig. 3. SEM images of (a) bare TiO₂, (b) MgO(2)_TiO₂, (c) MgO(10)_TiO₂, (d) MgO(30)_TiO₂, and (e) MgO(80)_TiO₂.

Table 1. EDS analysis of MgO modified TiO₂ thin films deposited on Ti foil

Sample	Atomic %		
	O	Ti	Mg
Bare_TiO ₂	66.16	33.83	0.01
MgO(2)_TiO ₂	63.23	36.66	0.11
MgO(10)_TiO ₂	71.35	28.24	0.41
MgO(30)_TiO ₂	73.48	24.51	2.01
MgO(80)_TiO ₂	74.08	16.76	9.16

ratio of Ti to O deviates from 1/2 as the thickness of MgO increases because the MgO deposited may block the signal of Ti from TiO₂.

For inspecting the crystallinity of the MgO modified TiO₂, X-ray diffraction analysis was used. The XRD patterns of various MgO modified TiO₂ on Ti foil are shown in Fig. 4. Pure MgO (250 nm) deposited on ITO glass, which was also measured, serves as the standard for MgO signals. Besides the Ti signal from the substrate, all the thin films exhibit anatase TiO₂ peaks, and only MgO(80)_TiO₂ shows a very small peak representing periclase MgO. This suggests that MgO with a thickness of less than 80 nm is insufficient to give a notable XRD signal, implying that the amount of MgO deposited on TiO₂ indeed is very small.

The UV-Vis absorption spectra of pure TiO₂ and MgO modified TiO₂ deposited on ITO glass are shown in Fig. 5. The pure TiO₂ thin film with a thickness of approximately 1,000 nm was fabricated by RFMS at room temperature. The MgO modified TiO₂

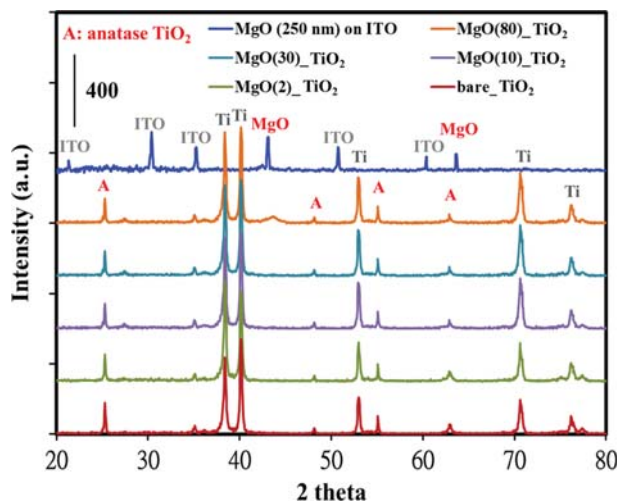


Fig. 4. XRD patterns of various MgO modified TiO₂ thin films prepared on Ti foil.

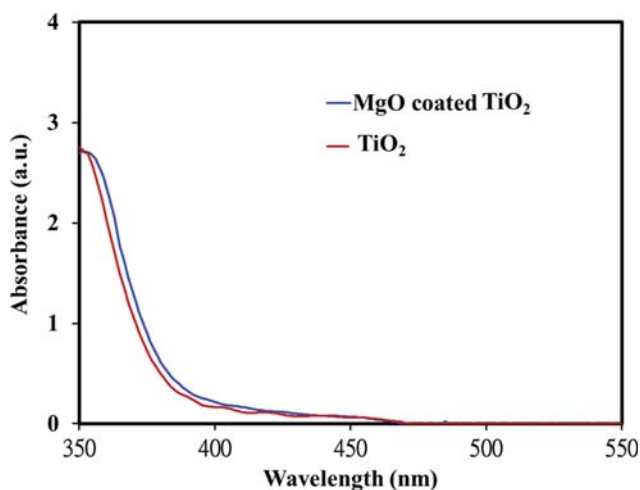


Fig. 5. UV-Vis absorption spectra of pure TiO₂ and MgO coated TiO₂ deposited on ITO.

thin film was fabricated by depositing 100 nm of MgO on pure TiO₂ with a total thickness of $\sim 1,100$ nm. From the result, the absorption of TiO₂ was observed at the wavelength of ~ 350 nm. The addition of MgO did not change the absorption spectrum of TiO₂ significantly. This confirms that MgO will not absorb light in the UV-Vis region due to its wide bandgap energy (8-9 eV) [22]. Regarding the optical properties of TiO₂/WO₃ film, it was revealed in our previous study [13]. It was demonstrated that the TiO₂/WO₃ film prepared by RFMS at a high temperature could absorb visible light and conduct the photocatalytic water splitting reaction under visible light. The detailed reason to make semiconductors absorb visible light is described by Prof. Anpo [23]. Under sputtering at high temperature, the O/Ti ratio gradually decreases from the top surface, leading to the perturbation in the electronic structure and the red-shift for the light absorption of TiO₂ [23]. To understand the hygroscopic properties of the MgO, the pure TiO₂ and MgO coated TiO₂ were deposited on glass, and the water contacting angle was also tested. As shown in Fig. 6, the pure TiO₂ surface has water

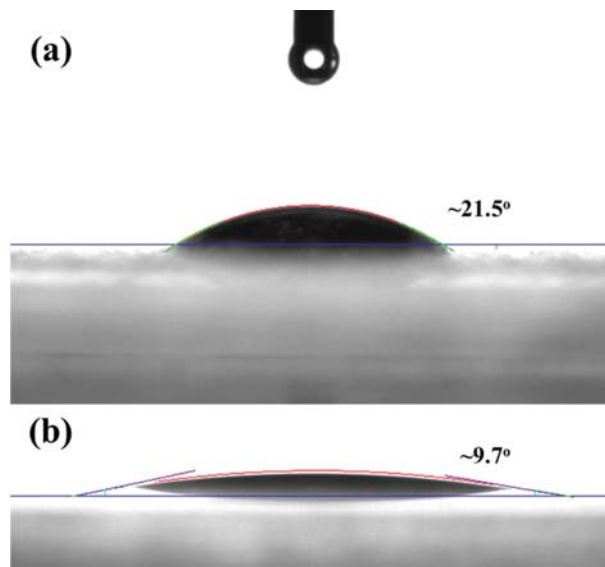


Fig. 6. Water contacting angles of (a) pure TiO₂ and (b) MgO coated TiO₂ deposited on glass.

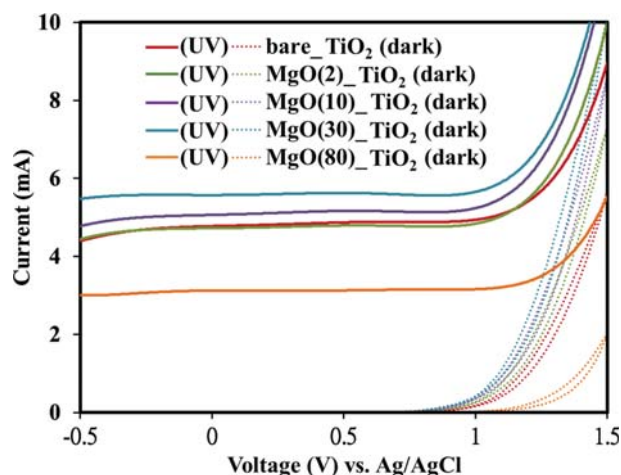


Fig. 7. CV plot of MgO modified TiO₂ thin films under UV irradiation.

contacting angle (WCA) of $\sim 21.5^\circ$, suggesting that the TiO₂ surface is hydrophilic (WCA $< 90^\circ$). After treating the TiO₂ with MgO, its surface becomes super-hydrophilic (WCA $< 10^\circ$) with WCA of $\sim 9.7^\circ$. This indicates that the coated MgO exhibits hygroscopic properties, which may adsorb more water molecules to favor oxidation of water and generation of oxygen.

The cyclic voltammograms (CVs) of MgO modified TiO₂ thin films under UV irradiation are shown in Fig. 7. For the results of CVs, the current density (mA/cm²) at the voltage of 0 V is listed in Table 2. It is noted that the photocurrent of the sample increased with MgO thickness up to 30 nm. When the MgO thickness further increased to 80 nm, the photocurrent of MgO modified TiO₂ dropped significantly. Therefore, it is concluded that coating a very thin layer of MgO on TiO₂ may have the benefit of improving TiO₂'s photoactivity. In this study, the optimal thickness of MgO was 30 nm. This conclusion is consistent with the result reported by Jung

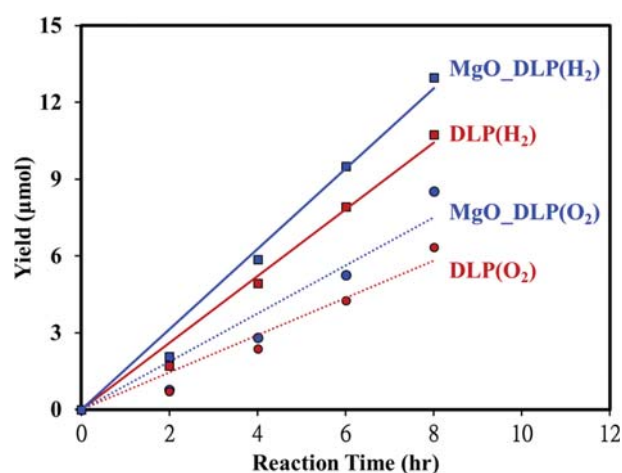
Table 2. Zero-voltage current density for MgO modified TiO₂ thin films

	Current density (mA/cm ²)				
	Bare_TiO ₂	MgO(2)_TiO ₂	MgO(10)_TiO ₂	MgO(30)_TiO ₂	MgO(80)_TiO ₂
Dark	2.3×10 ⁻⁴	2.4×10 ⁻⁴	2.9×10 ⁻⁴	2.0×10 ⁻⁴	3.9×10 ⁻⁴
UV	2.35	2.37	2.48	2.73	1.59
Net UV	2.35	2.37	2.48	2.73	1.59

et al. that coating a thin layer of MgO on TiO₂ can improve its photocatalytic activity towards the degradation of stearic acid [18]. They claimed that the improved photoactivity is due to the hygroscopic and nanoporous nature of MgO shell, which can absorb more water molecules and hydroxyl groups to form more hydroxyl radicals. The hygroscopic nature of MgO was evidenced by the FT-IR spectra between pure TiO₂ and MgO-coated TiO₂. However, since MgO is a wide-bandgap insulating material, too much of it may have a detrimental effect of blocking or suppressing the transport of charge carriers, resulting in reduced photoactivity.

Previously, it was demonstrated that TiO₂ thin film coated with 30 nm MgO exhibits the highest photoactivity in terms of photocurrent among the samples tested. Therefore, 30-nm MgO was selected to modify DLP, hoping to enhance the activity of photocatalytic water splitting. By conducting a photocatalytic water splitting reaction, the H₂ generation from DLP and MgO modified DLP (hereinafter referred to as MgO_DLP) was examined under light irradiation. The photocatalyst for the water-splitting reaction was noted as DLP or MgO_DLP/Ti/Pt (100 nm), as shown in Fig. 1(b). DLP was fabricated by depositing 2,440 nm of vis-TiO₂ on top of 560 nm vis-WO₃, while MgO_DLP was prepared by depositing 30 nm of MgO on top of DLP.

The results of H₂ and O₂ yields for DLP and MgO_DLP under visible-light irradiation are depicted in Fig. 8. As expected, the H₂ and O₂ yields of MgO_DLP are higher than those of DLP, being consistent with the photocurrent results. Note that the ratio of H₂-to-O₂ observed from the water-splitting reaction is not fully corresponding to the stoichiometric ratio of H to O in H₂O (2 to 1). The amount of H₂ generated was slightly lower than expected, especially at the initial stage of the photoreaction. We believe such a phenomenon is attributed to the fact that the H₂ produced initially was adsorbed/trapped on the Pt surface of the photocatalyst, making the ratio of H₂-to-O₂ low. It is also possible that part of the initial H₂ was consumed by reducing the surface PtO_x of the photocatalyst (cathode) since the Pt side was exposed in the air before the photoreaction. This argument is supported in advance by the results reported in our previous study, showing that the ratio of H₂-to-O₂ gradually returns to normal as the photoreaction continues over time [13]. Table 3 expresses H₂ and O₂ yields for both DLP and MgO_DLP in eight hours of visible-light irradiation. The

**Fig. 8. Water-splitting results for DLP and MgO_DLP under visible-light irradiation.**

MgO_DLP produced 12.98 μmoles H₂ and 8.54 μmoles O₂ while DLP generated 10.74 μmoles H₂ and 6.35 μmoles O₂. Comparing DLP, it is found that MgO_DLP exhibited an improvement of ~21% and ~35% for H₂ and O₂ yield, respectively. The efficiency of photon-to-hydrogen (PTH) was also obtained by Eq. (1), where P_{total} is the total power of incident light, Area is 2 cm² as preparation, and 237 kJ/mol is the Gibbs free energy for producing one mole H₂ from H₂O. The results of PTH are summarized in Table 3.

$$PTH = \left[\frac{(\mu\text{mol H}_2/\text{s}) \times (237 \text{ kJ/mol})}{P_{total} \left(\frac{\text{mW}}{\text{cm}^2} \right) \times \text{Area}(\text{cm}^2)} \right] \times 100\% \quad (1)$$

Similar to the photocurrent results, we believed that the improved H₂ and O₂ yields of MgO_DLP in water splitting are due to the hygroscopic nature of MgO [24], which can attract more water molecules toward the TiO₂ surface to perform water oxidation. Efficient water oxidation also means that fewer holes will be accumulated at the TiO₂-water interface to recombine with electrons; hence, H₂ yield is improved as well. Furthermore, we believed that MgO might provide more contacting surface area to hold

Table 3. H₂ and O₂ yields and PTH of DLP and MgO_DLP in 8 hours of visible-light irradiation

Light source	DLP			MgO_DLP		
	H ₂ yield (μmole)	O ₂ yield (μmole)	PTH (%)	H ₂ yield (μmole)	O ₂ yield (μmole)	PTH (%)
Visible light	10.74	6.35	0.044	12.98	8.54	0.053

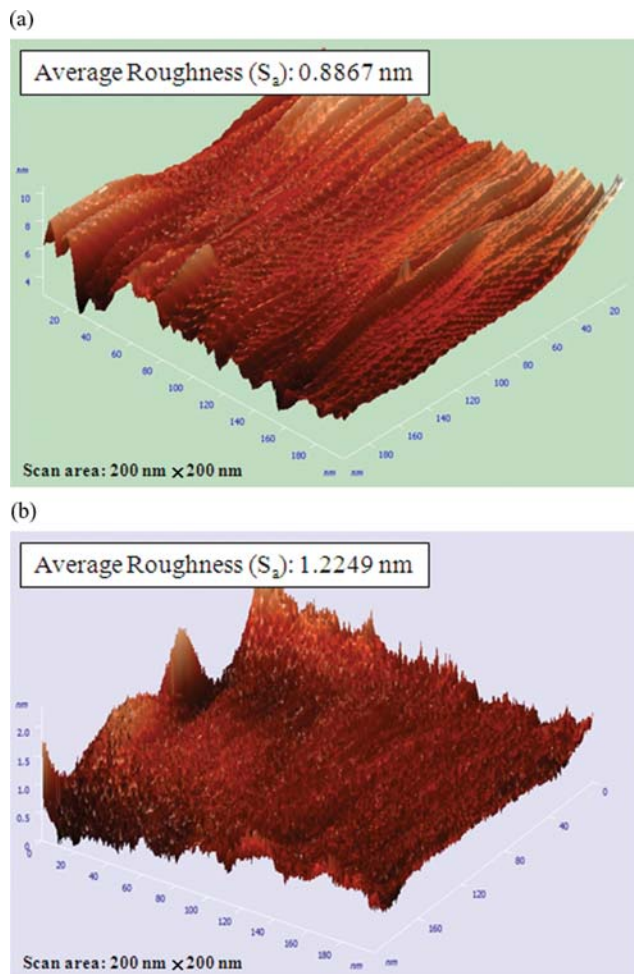


Fig. 9. AFM images of (a) bare TiO_2 and (b) MgO-coated TiO_2 .

more water molecules for water oxidation, as reported in the literature [18]. Since it is difficult to measure the specific surface area of thin film by the conventional BET (Brunauer-Emmett-Teller) method, AFM was adopted to examine the contacting surface area of thin films based on their surface roughness, because in general the rough surface tends to have larger contacting surface area than smooth surface. AFM analysis was performed on bare TiO_2 and MgO-coated TiO_2 thin films. Bare TiO_2 was prepared by sputtering 1,000 nm of TiO_2 on ITO glass, whereas MgO-coated TiO_2 was prepared by sputtering an additional layer of MgO (30 nm) on top of bare TiO_2 . The AFM images of both samples are shown in Fig. 9. It appears that MgO-coated TiO_2 has higher surface roughness than bare TiO_2 . The calculated average surface roughness (S_a) for bare TiO_2 and MgO-coated TiO_2 is 0.8867 and 1.2249 nm, respectively, implying that MgO-coated TiO_2 has a higher contacting surface area. Based on this result, it can be concluded that the inclusion of MgO will provide more contacting surface area for the absorption of water molecules on the TiO_2 surface. From the water-splitting results, the mechanism of MgO preventing electrons from reducing water molecules at the TiO_2 -water interface was proposed, as shown in Fig. 10. As a result, MgO served as an insulator may suppress current leakage by preventing electrons from reduc-

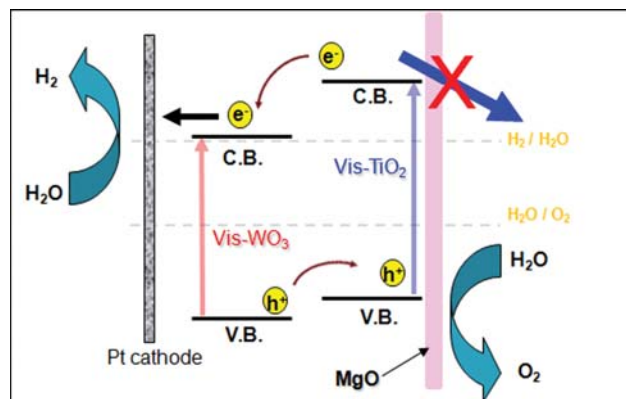


Fig. 10. Schematic diagram of MgO preventing electrons from reducing water molecules at the TiO_2 -water interface.

ing water molecules at the TiO_2 -water interface.

CONCLUSION

The effect of adding a thin layer (or small amount) of MgO on TiO_2 was investigated. It was noted that the inclusion of MgO did not change the absorption spectrum of TiO_2 significantly. This confirmed that MgO will not absorb light in the UV-Vis region due to its wide bandgap energy (8-9 eV). From the photocurrent measurement results, it was found that coating a very thin layer of MgO on TiO_2 may have the benefit of improving TiO_2 's photoactivity. The optimal thickness of MgO in this study was 30 nm, estimated from the calibration curve. Finally, DLP was modified by 30 nm of MgO and its photoactivity towards H_2 production was investigated by carrying out the photocatalytic water-splitting reaction in the twin-cell reactor under visible-light irradiation. Compared with regular DLP, MgO_DLP can generate 12.98 μmoles H_2 and 8.54 μmoles O_2 after 8 hours of reaction. It shows an improvement of $\sim 21\%$ and $\sim 35\%$, respectively, for H_2 and O_2 yield. We believe that the improved H_2 and O_2 yields of MgO_DLP are due to the hygroscopic nature of MgO, which can attract more water molecules towards the TiO_2 surface to perform water oxidation. Consequently, fewer holes will be accumulated at the TiO_2 -water interface to recombine with electrons, improving the H_2 yield simultaneously. Moreover, incorporation of a thin layer of MgO on DLP can also suppress the photocatalyst's current leakage by preventing electrons from reducing water molecules at the TiO_2 -water interface.

ACKNOWLEDGEMENTS

This study was supported under grant number MOST 105-2221-E-002-206-MY3, 106-2218-E-992-304-MY2, and 108-3116-F-006-013 from the Ministry of Science and Technology (MOST), Taiwan. The authors also appreciate the Academia Sinica of Taiwan for partial support under the project AS-KPQ-106-DDPP.

REFERENCES

1. M. Momirlan and T. N. Veziroglu, *Renew. Sust. Energy Rev.*, **6**, 141

- (2002).
2. M. Ni, M. K. H. Leung, D. Y. C. Leung and K. Sumathy, *Renew. Sust. Energy Rev.*, **11**, 401 (2007).
 3. A. Fujishima and K. Honda, *Nature*, **238**, 37 (1972).
 4. C.-W. Huang, V.-H. Nguyen, S.-R. Zhou, S.-Y. Hsu, J.-X. Tan and K. C. W. Wu, *Sustain. Energy Fuels*, **4**, 504 (2020).
 5. S. G. Kumar and L. G. Devi, *J. Phys. Chem. A*, **115**, 13211 (2011).
 6. R. Asahi, T. Morikawa, T. Ohwaki, K. Aoki and Y. Taga, *Science*, **293**, 269 (2001).
 7. K. Domen, A. Kudo, T. Onishi, N. Kosugi and H. Kuroda, *J. Phys. Chem.*, **90**, 292 (1986).
 8. K. Gurunathan, P. Maruthamuthu and M. V. C. Sastri, *Int. J. Hydrogen Energy*, **22**, 57 (1997).
 9. A. Kudo, H. Kato and S. Nakagawa, *J. Phys. Chem. B*, **104**, 571 (1999).
 10. H. Kikuchi, M. Kitano, M. Takeuchi, M. Matsuoka, M. Anpo and P. V. Kamat, *J. Phys. Chem. B*, **110**, 5537 (2006).
 11. M. Kitano, M. Takeuchi, M. Matsuoka, J. M. Thomas and M. Anpo, *Chem. Lett.*, **34**, 616 (2005).
 12. C. H. Liao, C. W. Huang and J. C. S. Wu, *Int. J. Hydrogen Energy*, **37**, 11632 (2012).
 13. C. H. Liao, C. W. Huang and J. C. S. Wu, *Asia-Pac. J. Chem. Eng.*, **8**, 283 (2013).
 14. M. Kitano, M. Takeuchi, M. Matsuoka, J. A. Thomas and M. Anpo, *Catal. Today*, **120**, 133 (2007).
 15. H. Tada, Y. Kubo, M. Akazawa and S. Ito, *Langmuir*, **14**, 2936 (1998).
 16. H. Tada, M. Yamamoto and S. Ito, *Langmuir*, **15**, 3699 (1999).
 17. C. Anderson and A. Bard, *J. Phys. Chem.*, **99**, 9882 (1995).
 18. H. S. Jung, J. K. Lee, M. Nastasi, J. R. Kim, S. W. Lee, J. Y. Kim, J. S. Park, K. S. Hong and H. Shin, *Appl. Phys. Lett.*, **88**, 013107 (2006).
 19. S.-T. Bae, H. Shin, J. Y. Kim, H. S. Jung and K. S. Hong, *J. Phys. Chem. C*, **112**, 9937 (2008).
 20. C. W. Huang, C. H. Liao, J. C. S. Wu, Y. C. Liu, C. L. Chang, C. H. Wu, M. Anpo, M. Matsuoka and M. Takeuchi, *Int. J. Hydrogen Energy*, **35**, 12005 (2010).
 21. C. H. Liao, C. W. Huang and J. C. S. Wu, *Int. J. Hydrogen Energy*, **37**, 11632 (2012).
 22. H. S. Jung, J.-K. Lee, M. Nastasi, S.-W. Lee, J.-Y. Kim, J.-S. Park, K. S. Hong and H. Shin, *Langmuir*, **21**, 10332 (2005).
 23. M. Kitano, H. Kikuchi, T. Hosoda, M. Takeuchi, M. Matsuoka, T. Eura, M. Anpo and J. M. Thomas, *Key Eng. Mater.*, **317**, 823 (2006).
 24. H. S. Jung, J. K. Lee, K. S. Hong and H. J. Youn, *J. Appl. Phys.*, **92**, 2855 (2002).